Applied Surface Science 631 (2023) 157498

Contents lists available at ScienceDirect

Applied Surface Science

journal homepage: www.elsevier.com/locate/apsusc

Full Length Article

Changes in fundamental and catalytic properties of β-molybdenum carbide decorated by a single atom of Fe, Co, Ni and Cu

Andrey A. Koverga [a,*], Ana M. Gómez-Marín [b], Elizabeth Flórez [c], Edson A. Ticianelli [a]

[a] Instituto de Quimica de São Carlos, Universidade de São Paulo, 13560-960 São Carlos, SP, Brazil
[b] Department of Chemistry, Division of Fundamental Sciences, Technological Institute of Aeronautics, 12228-900 São Jose dos Campos, SP, Brazil
[c] Grupo de Investigacion Mat&mpac, Facultad de Ciencias Básicas, Universidad de Medellín, Medellín, Colombia

ARTICLE INFO

Keywords:
DFT
Molybdenum carbide
Adatom decoration
Doping
HER

ABSTRACT

The interaction of single Fe, Co, Ni, and Cu atoms with polar terminations of orthorhombic $Mo_2C(001)$ surface has been investigated at low surface coverage by using density functional theory. Calculations indicate high stability of all considered adsorbates, regardless the surface termination. The presence of a single foreign atom has a localized impact on the properties of the surface, causing charge redistribution in the adsorbate/surface interface. As the result lowering of the work function is observed for both $Mo_2C(001)$ terminations. Another effect is shifting the position of *d*-band center further away from the Fermi level for surface Mo atoms of metal-terminated carbide, while no changes are seen for carbon's near-Fermi level electronic states in the case of C-terminated modified surface. Results demonstrate a short-range effect on the stability of atomic hydrogen caused by the foreign adatom on both terminations. Specifically, the observed adsorption energy weakening would entail an enhancement in the catalytic activity of Mo_2C toward hydrogen evolution reaction according to the Sabatier principle. Results evidence that molybdenum carbide modified by cobalt and iron is expected to be more active toward hydrogen evolution reaction than Mo_2C modified by nickel and copper or than unmodified carbide.

1. Introduction

Growing concerns about the ongoing energy crisis and environmental pollution raise a demand for clean and efficient methods of energy conversion and storage. The high power density of hydrogen [1] makes it an attractive environmentally friendly alternative to carbon-based energy carriers. Although hydrogen is the most common element in the Universe, it is not readily available in a free form. The majority of hydrogen nowadays is obtained from a water–gas shift reaction with CO_2 as a by-product, thus, urging a search for more "green" production strategies.

Electrochemical water splitting presents a viable pollution-free way of hydrogen synthesis. However, one of the challenges for the mass-implementation of this method is the high cost of current catalysts for the hydrogen evolution reaction (HER) (Eq.1) [2–5].

$$2H^+ + 2e^- \rightarrow H_2 \text{ (acidic media)} \quad (1)$$

$$2H_2O + 2e^- \rightarrow H_2 + 2OH^- \text{ (alkaline media)}$$

After decades of searching, Pt-based materials are still the most efficient catalysts for the HER [2,3,5–7]. However, due to their scarcity and high pricing, alternative catalysts must be sought. Additionally to the low price for alternative materials, another requirement is high stability in typical working conditions of HER, since low stability further increases the cost of these technologies.

Since the seminal work of Levy and Boudart reporting "Pt-like" catalytic properties of tungsten carbide toward selected processes,[8] transition metal compounds attracted a lot of interest as a possible cost-effective alternative to noble metal-based catalysts [9–17] and molybdenum-based materials emerged as promising catalysts for HER [3,10,18–26]. However, their catalytic activity is lower than that of Pt-based catalysts, and, therefore, needs careful and systematic tailoring to attain acceptable levels for application in practical systems.

Previous studies concluded that HER activity of molybdenum carbide can be altered by modifying it with other transition metals, such as Fe, Co, Ni, and Cu [27–30]. These works analysed the overall effect of molybdenum carbide doping with transition metals that include both surface adsorption and insertion of the foreign atom into the crystalline

* Corresponding author.
E-mail address: a.koverga@usp.br (A.A. Koverga).

https://doi.org/10.1016/j.apsusc.2023.157498
Received 14 February 2023; Received in revised form 19 April 2023; Accepted 9 May 2023
Available online 13 May 2023

lattice of the host material. The impact of the dopants on the HER activity of the parent material was explained in terms of a charge transfer from the dopant metal to adjacent atoms of the carbide, that modifies the *d*-electron configuration of Mo_2C particles and affects the oxidation state and average bond ionicity.

Nevertheless, the exact impact of transition metal atoms on the electronic and catalytic properties of molybdenum carbide remains unclear. Here, it must be noted that catalytic properties of a given material can be altered through modification of its surface by adsorption of foreign atoms, or adatoms [31–37]. Upon adatom adsorption the formation of heteroatom bonds (ligand effect), or changes in the average atom–atom bond length (strain effect) may result in a shift of various fundamental properties of the host material, which in turn affects its catalytic activity toward target processes. On well-defined surfaces, this method also offers insights into the surface chemical environment at the atomic level during (electro)chemical reactions, such as adlayer's structure, availability/nature of active surface sites, and in general aids to unravel complex relationships between surface structure, composition, and reactivity.

Numerous studies are available on the modification of transition metal carbides with other metals [2,38–45]. They, however, concern about the properties of the supported metal adlayer, rather than of the host carbide material. A density functional theory-based study of Fe, Co, Ni, and Cu single atom interaction with model molybdenum carbide surfaces would present a first step toward a better understanding of the changes in fundamental properties of molybdenum carbide upon modifying it with other transition metals. Experimental studies have clearly demonstrated the effect of these particular metals on the carbide's HER activity, but their specific impact on Mo_2C electronic properties is still not known. This fact, combined with the availability of these metals for practical implementation, makes them a valuable subject for a theoretical study, which could offer deeper insights into the reasons behind the experimentally observed shift in catalytic properties of modified molybdenum carbide toward HER. Furthermore, it can present a useful basis for the functional design of materials with a set of characteristics, optimized for the target electrochemical reaction.

This work, therefore, aims to explore modification of the work function, charge distribution, and electronic structure of orthorhombic $Mo_2C(001)$ surface caused by the adsorption of a single atom of cobalt, copper, iron, and nickel at low surface coverage. The orthorhombic molybdenum carbide phase was selected because of its higher stability, compared to hexagonal one [46–48]. In its turn, the choice of (001) plane is dictated by the fact that its polar C- and Mo-terminations possess distinctive fundamental properties,[42,44,46] and, therefore, are expected to interact differently with the adatoms. Hence, the study of adatom interaction with these polar terminations allowed to obtain a more complete picture on the changes in fundamental properties of the carbide upon modifying it with other transition metals. By considering the interaction of only one adsorbed atom this study was able to focus on the evolution of the characteristics of the carbide itself, rather than on the properties of the adatom layer.

Observed adatom-induced modifications of these fundamental properties were then reviewed in the context of their impact on single hydrogen atom interaction with polar terminations of the carbide, allowing to elucidate the effect of the adatoms on the catalytic performance of the modified carbide toward HER.

2. Computational details

Spin-polarized calculations were performed using Vienna *ab initio* simulation package (VASP) [49–52]. Exchange correlation interactions were treated with the generalized gradient approximation by Perdew, Burke and Ernezerhof [53]. The Projector Augmented Wave core potentials,[54] as implemented in VASP by Kresse and Joubert[55] were used. In all cases a cut-off for the plane-wave basis set of 415 eV was applied. To improve the description of the long-range correlation effects, especially for systems with adsorbed hydrogen, the dispersion correction proposed by Grimme,[56] namely its D3 scheme,[57] was used.

A dipole correction scheme was applied in all cases to ensure that slabs, repeating in the direction perpendicular to the surface plane, were electronically decoupled. Integration of the reciprocal space for all surfaces was performed using the Monkhorst-Pack scheme[58] with a 3 × 3 × 1 k-points sampling – for geometry optimization procedures, and 11 × 11 × 1 – for the Density of States calculations. First order Methfessel-Paxton approach[59] with a Gaussian width of smearing of 0.2 eV was applied to smear the Fermi level. When required, single atom calculations in the gas phase were performed using a similar set of parameters, in a cubic 8 Å × 8 Å × 8 Å cell with a single Gamma point sampling. The bulk structure was obtained by minimizing the total energy of the unit cell, optimizing both lattice vectors and atomic coordinates, using the Newton–Raphson algorithm similarly to previously reported studies [46,60].

It must be noted here that the nomenclature defined by the Joint Committee of Powder Diffraction Standards (JCPDS)[46] was used. Thus, in this work the orthorhombic phase of molybdenum carbide is referred to as β-Mo_2C. Specifically, polar metal and carbon terminations of β-$Mo_2C(001)$ surface were considered. Iron, nickel, cobalt and copper were used as modifying transition metals (TM).

Model (001) surfaces were created from optimized bulk structures. Orthorhombic molybdenum carbide surfaces were represented by (4 × 4) supercell consisting of 8 alternating Mo and C atomic layers, with 14 Å of vacuum separating repeating images in the direction perpendicular to the surface plane. The upper layer for C-terminated β-$Mo_2C(001)$, denoted in this work as C-Mo_2C, contained 8 carbon atoms and 16 Mo atoms in the sublayer, and Mo-terminated β-$Mo_2C(001)$, or Mo-Mo_2C, contained 16 Mo atoms in the topmost layer (Fig. 1). For structure optimization four upper layers were allowed to relax simultaneously with the adsorbate species present on the surface, while the bottom four were frozen in a bulk-like geometry. The convergence criterion was met when the variation in the total forces were smaller than 0.01 eV/Å at the current and previous step.

Modification of polar terminations of $Mo_2C(001)$ surface with a single TM atom was analysed on two types of top, bridge and three-fold hollow sites on C-$Mo_2C(001)$, and atop of Mo atom, on bridge and three different three-fold hollow sites on Mo-$Mo_2C(001)$, as illustrated in Fig. 1. The most stable adsorption site for the TM adatoms on both Mo_2C (001) terminations was established by selecting the systems for which the most negative adsorption energy was calculated:

$$E_{Ads} = E_{TM/Mo_2C} - E_{TM.g} - E_{Mo_2C} \quad (2)$$

E_{TM/Mo_2C} here is the total energy of system with carbide surface and TM adatom, $E_{TM.g}$– energy of a single adatom in gas phase and E_{Mo_2C} – energy of corresponding pristine carbide termination.

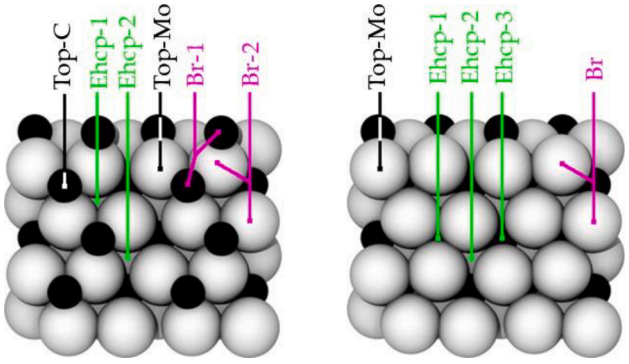

Fig. 1. Top view on C-$Mo_2C(001)$ and Mo-$Mo_2C(001)$ with indicated adsorption sites available on these surfaces for interaction with Fe, Co, Ni and Cu atoms or atomic hydrogen. Molybdenum and carbon are represented by silver and black spheres, respectively.

These relatively large supercells enabled the study of the impact of the TM adatom on fundamental properties of the host surfaces, with minimal possible lateral interactions of modifying atoms in the repeating cells. Resulting low coverage of the TM adatoms, $\Theta_{TM} = 1/16$ ML, additionally, allowed to verify whether the effect of TM presence in molybdenum carbide was localized and estimate its region of impact.

This setup also enables an analysis of atomic hydrogen interaction with pristine and TM-modified molybdenum carbide surfaces at a low coverage, which is essential for a theoretical evaluation of the catalytic activity of materials toward hydrogen evolution reaction (HER) [44]. Similar model setup, although with lesser total number of atomic layers, has proven to be sufficient to obtain reproducible results for carbide-based systems,[46,61] specifically those, that include interaction of other metals with the carbides. [41,42,44,45] Interaction sites with atomic H were established for each termination of the $Mo_2C(001)$ surface. For this, hydrogen binding energy (HBE), was calculated for C- and Mo-Mo_2C surfaces as.

$$E_{Ads,H} = E_{Surf+H} - E_{Surf} - \frac{1}{2}E_{H_{2,g}} \quad (3)$$

here E_{Surf+H}, E_{Surf} and $E_{H_{2,g}}$ are total energies of molybdenum carbide surface with H atom on it, of pristine Mo_2C termination and of hydrogen molecule in the gas phase, respectively. Calculated HBE values for pristine $Mo_2C(001)$ surface terminations were −0.87 eV and −1.15 eV on the Top-C site of C-Mo_2C and Ehcp-1 site of Mo-Mo_2C systems, respectively (see Fig. 1). These data are in good agreement with the reported stable sites for H atom and HBE (-3.17 eV and −3.17 eV, if total energy if a single H atom in gas phase is used as the reference, or −0.92 eV and −1.06 eV if $\frac{1}{2}E_{H_{2,g}}$ is used), calculated for these surfaces, using the vdW corrections [62].

HBE values on TM-modified Mo_2C surfaces were obtained in the same fashion, as the difference in total energy of the modified Mo_2C surface with H atom on it and the sum of total energy of corresponding clean surface and half total energy of H_2 molecule in the gas phase.

The work function, Φ, for all studied surfaces was obtained as the difference between the potential of the vacuum region,V_∞, and the Fermi level, E_F, of the surface:

$$\Phi = V_\infty - E_F \quad (4)$$

Bader charge analysis [63] has been performed on TM-modified molybdenum carbide surfaces as implemented in VASP by Henkelman, Arnaldsson and Jónsson [64]. The total net charge for molybdenum, carbon, hydrogen and TM atoms was calculated as.

$$Q_X = Z_X - q_{Bader,X} \quad (5)$$

where Z_X is the number of valence electrons and $q_{Bader,X}$ is the calculated Bader charge for the corresponding X atom.

The charge density difference (CDD) was calculated as.

$$\Delta\rho = \rho_{TM/Mo_2C} - \rho_{Mo_2C} - \rho_{TM} \quad (6)$$

here ρ_{TM/Mo_2C} is the charge distribution in the modified molybdenum carbide, ρ_{Mo_2C} – is the charge distribution for the carbide surface frozen in the geometry it has in the TM-modified structure and ρ_{TM} is the charge distribution of the isolated TM atom in the gas phase occupying the same coordinates in space as it has in the TM-modified system. The rearrangement of charge can be visualized by plotting the laterally averaged charge density profile, which corresponds to the lateral sum of the charge density difference in the *x* and *y* directions, according to

$$\Delta\rho_{ave} = \iint_{cell} \Delta\rho \, dx \, dy \quad (7)$$

The *d*-band center for Mo atoms, was calculated as first moment of the projected *d*-band density of states, ρ_d in respect to the Fermi level:

$$\varepsilon_d = \frac{\int_{-\infty}^{\infty} E\rho_d(E - E_F)dE}{\int_{-\infty}^{\infty} \rho_d(E - E_F)dE} \quad (8)$$

3. Results and discussion

Molybdenum carbide has been the subject of numerous theoretical studies, focusing on fundamental properties of different phases and surfaces [46,60,65–68]. To assure that the model used in the present study correctly describes β-Mo_2C, its bulk properties were calculated using the setup described in Section 2 and are summarized in Table S1 of the Supplementary Information, together with experimental and theoretical data, available in the literature. It is seen that the calculated properties are in good agreement with previously reported experimental studies[65,69,70] and theoretical data, obtained with PBE[46,66] and PW91 functionals [60]. Small differences seen between theoretical and experimental data can be attributed to the imperfect nature of molybdenum carbide phase that calculations usually do not account for [12].

3.1. Properties of C-$Mo_2C(001)$ and Mo-$Mo_2C(001)$ surfaces, modified with other TM atoms

3.1.1. General properties.

Interaction of single Fe, Co, Ni and Cu adatom with model C-Mo_2C and Mo-Mo_2C surfaces was studied by placing the TM atom on the adsorption sites, presented in Fig. 1 at initial distance ~ 1.6 Å and relaxing these systems. Similarly to previously reported data on adsorption of Pt and Cu on polar termination of the $Mo_2C(001)$ surface, [42,44] after the relaxation, all TM adatoms were found to adsorb on the Ehcp-1 site of the C-Mo_2C system. On the Mo-terminated surface the Ehcp-2 site was the most stable one, regardless of the nature of the adatom. Characteristics for the stable TM/Mo_2C systems, including adsorption energies of the adatoms and charge distribution in the TM–Mo_2C contact region, are summarized in Table 1.

In all considered systems strong TM–Mo_2C interaction takes place, judging from the values of E_{Ads}, more so on C-terminated surface. Interestingly, on C-Mo_2C surface Fe and Co adatoms were found to be significantly more stable than Ni and Cu, although even the weakest adsorption of copper on this surface is characterized by a large E_{Ads} value of −3.97 eV. On Mo-Mo_2C the E_{Ads} values are closer to one another, and all adatoms are almost equally stable with the exception of copper, for which its adsorption is at least 1.2 eV weaker than for the rest of the considered TM species.

For each TM cohesion energy of corresponding bulk structure, can calculated as $E_c = \frac{E_{TM_n} - nE_{TM}}{n}$, where E_{TM_n} and E_{TM} are total energies of a cell containing *n* TM atoms organized in bulk geometry and isolated TM atom, resp. By comparing the obtained E_{Ads} for a TM atom with respective bulk cohesion energy a conclusion can be made whether the single TM atom adsorption is more or less energetically favourable than this atom incorporating into the bulk metal structure. From the data summarized in Table 2 it is evident that in all cases adsorption of a single TM atom is more likely to occur than this atom “joining” bulk structure of the respective TM.

To the knowledge of the authors, little information on interaction of either a single atom of the considered TM species or their clusters with the Mo_2C surfaces is available in the literature. A study of the interaction of Cu monolayer and clusters of various sizes with polar terminations of $Mo_2C(001)$ [42] and WC(0001)[40] demonstrated that Cu adsorption on C-terminated surface is more stable than on metal termination of the transition metal carbides, in agreement with the trends observed for Fe, Co, Ni and Cu adsorption in the present work. An opposite termination-dependent trend for E_{Ads} was observed for Pt on Mo_2C[44] and WC, [40,41,44] where on both carbides it was more stable on their metal terminations.

Also, although adsorption energies reported in the mentioned studies

Table 1
Standard redox potentials ($E^{o}_{TM^{z+}/TM}$), calculated TM bulk cohesion energies (E_c), adsorption energies (E_{Ads}), distance between the TM and surface plane (d⊥), average Mo–Mo and Mo–C distances in the vicinity of the adatom (d_{Mo-Mo} and d_{Mo-C}, resp.), Bader charges for Mo (Q_{Mo}) and C (Q_C) atoms closest to the foreign atom and for the TM atom (Q_{TM}), calculated for C-Mo_2C(001) and Mo-Mo_2C(001) surfaces decorated by the TM adatoms.

System	TM	$E^{o}_{TM^{z+}/TM}$(V)	E_c (eV)	E_{Ads} (eV)	d⊥ (Å)	$d_{Mo—Mo}$ (Å)	$d_{Mo—C}$ (Å)	Q_{Mo} (*e*)	Q_C (*e*)	Q_{TM} (*e*)
C-Mo_2C	Fe	−0.44	−4.28	−6.32	0.89	3.00	2.10	+1.59	−2.11	+0.69
	Co	−0.28	−4.42	−6.39	0.88	3.01	2.09	+1.60	−2.02	+0.46
	Ni	−0.23	−4.51	−5.89	0.92	2.98	2.09	+1.60	−2.01	+0.48
	Cu	+0.34	−3.48	−4.14	0.95	3.00	2.05	+1.75	−1.99	+0.37
Mo-Mo_2C	Fe	−0.44	−4.28	−5.22	1.72	3.04	2.08	+1.23	−2.48	−0.56
	Co	−0.28	−4.42	−5.53	1.68	3.08	2.09	+1.26	−2.49	−0.43
	Ni	−0.23	−4.51	−5.61	1.61	3.15	2.09	+1.24	−2.47	−0.64
	Cu	+0.34	−3.48	−3.99	1.80	3.17	2.10	+1.19	−2.49	−0.69

Table 2
Adsorption energy ($E_{ads,H}$), position of H atom in respect to the TM adatom (H location), shortest H–surface distance (d⊥(H-Surf)) and distance between H and the TM (d(H-TM)) and Bader charge values (Q_H) for atomic hydrogen adsorbed on the TM-modified Mo_2C surfaces close and far to the modification site.

System	H location	$E_{ads,H}$ (eV)	d⊥(H-Surf) (Å)	d(H-TM) (Å)	Q_H (*e*)
Fe/C-Mo_2C	Close	−0.55	1.11	2.52	+0.14
	Far	−0.79	1.10	6.53	+0.18
Co/C-Mo_2C	Close	−0.53	1.11	2.47	+0.15
	Far	−0.82	1.10	6.62	+0.19
Ni/C-Mo_2C	Close	−0.78	1.11	2.42	+0.13
	Far	−0.84	1.10	6.77	+0.19
Cu/C-Mo_2C	Close	−0.70	1.11	2.44	+0.19
	Far	−0.84	1.10	6.60	+0.19
Fe/Mo-Mo_2C	Close	−0.83	1.03	2.00	−0.64
	Far	−1.14	1.04	4.89	−0.71
Co/Mo-Mo_2C	Close	−0.83	1.05	1.96	−0.60
	Far	−1.14	1.04	4.84	−0.70
Ni/Mo-Mo_2C	Close	−0.92	1.03	2.02	−0.61
	Far	−1.15	1.05	4.82	−0.71
Cu/Mo-Mo_2C	Close	−0.93	1.02	2.27	−0.69
	Far	−1.16	1.05	4.86	−0.71
C-Mo_2C	–	−0.87	1.11	–	+0.19
Mo-Mo_2C	–	−1.15	1.04	–	−0.71

were obtained for multi-atom clusters, the clear tendency of E_{Ads} per atom decreasing with the growing number of Cu adatoms in the Cu/Mo_2C system allows to assume that single Cu atom adsorption should be more stable than that of the cluster containing several atoms. Indeed, calculated E_{Ads} values for a single copper atom evidence its higher stability on both carbide terminations, compared to the energy reported for the multi-atom cluster [42].

For the same TM species, depending on the termination of the Mo_2C (001) surface, a variation is seen for the adatom – surface plane distances (d⊥, Table 1). Similarly to the observations made for Pt single atom interacting with polar terminations of the WC (0001) and Mo_2C (001),[44] adatoms adsorb further from metal-terminated surface than from C-terminated one. By comparing the distances between the TM and surface plane for all systems it is found that on C-Mo_2C, cobalt and iron come closest to the surface upon adsorption, compared to the rest of the adatoms, while nickel – surface distance is the largest. A somewhat different tendency is seen on metal-terminated surface, where nickel adatom is the closest to the surface, while copper is the furthest from the surface, compared to the rest of the TM.

The TM adatom presence has an effect on average Mo–C distances in the region closest to the adatom that depends on the carbide's termination. On C-terminated surface an increase is universally seen from the average distance of 1.98 Å (Table S2) in the upper layers of the unmodified system, regardless of the nature of the adsorbate. In the TM/Mo-Mo_2C systems the calculated Mo–C distances remain close to the value of 2.08 Å of the unmodified Mo-Mo_2C.

Distances between neighbouring molybdenum atoms are also affected by adsorption of the TM atoms: regardless of nature of the TM or termination of the carbide, a slight metal layer contraction is seen in the proximity of the adatom, from initial values of 3.10 Å and 3.18 Å calculated for C- and Mo-terminated surfaces, respectively (Table S2). This effect is more noticeable for TM/C-Mo_2C systems, where the average reduction in the bond length was ~ 0.1 Å, and less so for TM/Mo-Mo_2C systems, for which Ni and Cu adatoms have little to no effect on the structure of the topmost layer, and presence of Co and Fe results in a 0.10 Å and 0.14 Å shorter Mo–Mo distances, respectively, compared to the clean surface.

These adatom-induced changes in geometry of the metal layers of the substrate, may entail important modifications on the local electronic structure of the surface [71,72]. For purely metallic systems these changes are expected to locally affect catalytic activity in the proximity of the adatom toward certain processes,[41,73,74] through modification of electronic states of the surface atoms in the adatom–surface contact region. For more complex systems, such as TM-modified carbide, the impact of the "strain" on their catalytic properties is not that straightforward, because of difference in chemical and catalytic properties of their polar terminations and active sites present on them. For instance, while for C-Mo_2C the TM-induced contraction would probably affect the *d*-band center of Mo atoms in the adatom proximity, this particular change will have a little to none impact on the interaction of atomic hydrogen with the surface at low H coverages, since H preferably interacts with surface carbon atoms [44,62]. At the same time, on Mo-Mo_2C, where atomic hydrogen interacts with surface molybdenum atoms, this effect would play a more important role, since surface Mo properties may be affected by the adatom.

3.1.2. *Electron localization and charge distribution.*

Analysis of electron localization function (ELF) plots (Fig. S1) showed that the termination of the support plays an important role in the formation of the bond between the TM adsorbate and the carbide. Evidently, on both terminations the TM—Mo_2C bond has a mixed covalent-metallic nature, regardless of the nature of the adsorbing species. However, the TM/Mo-Mo_2C systems are characterized by a high concentration of electrons in the region between the TM adatom and surface Mo atoms, while in the TM/C-Mo_2C electrons are localized close to the surface carbon atoms. This leads to the conclusion that on Mo-terminated surfaces the nature of the TM—Mo interaction is rather metallic, while on C-terminated surface the TM—C bond is more covalent. The ELF plots also evidence that adatoms interact only with the surface atoms in their vicinity, pointing to the local nature of any impact that the TM adsorbates would have on fundamental properties of the carbide.

The charge transfer is an important component in surface–adatom bonding, often defining chemical properties of the supported particle and exposed sites of the support [43,44,75–78]. In practical electrochemical systems, charge transfer can also affect the structure of the electric double layer and the distribution of Galvani potential [79] close to the electrode. It is important to highlight that predicting the magnitude of the charge transfer is not a straightforward task, especially for complex systems as carbides, since they are composed of atoms with

different electronegativity, such as carbon and molybdenum.

From a Bader charge analysis (see Table 1) it is clear that the total net charge on TM adatoms significantly depends on the termination of the support. On C-terminated $Mo_2C(0\,0\,1)$ all adatoms are charged positively (*i.e.* adatom → surface charge transfer takes place), while on the Mo-terminated surface the opposite picture is seen. Similar observations have also been made for Cu clusters supported on polar terminations of WC(0001)[43] and $Mo_2C(0\,0\,1)$[42] and for Pt supported on polar terminations of WC(0001) and $Mo_2C(0\,0\,1)$ [44]. In these two systems, only the charge on the atoms that are closest to the adatom are affected by its presence, while the rest of molybdenum and carbon atoms in the upper two layers of each surface retain their original charges. This charge distribution is in good agreement with the results seen in the electron localization function plots, discussed above.

It is noteworthy that on C-Mo_2C surface the positive charge on the adatom is decreasing in order Fe > Ni > Co > Cu, while on Mo-Mo_2C the net negative charge on the TM adatoms increases in the row Co > Fe > Ni > Cu. In the first case, the trend for Fe, Co and Cu follows what would be expected from differences in electronegativity of these elements (Ni ($\chi = 1.91$) > Cu ($\chi = 1.90$) > Co ($\chi = 1.88$) > Fe ($\chi = 1.83$)[80]) and C ($\chi = 2.55$), indicating that electronegativity of the adatoms plays an important role in the charge transfer upon interaction of the TM with the carbide support. Within the Bader charge partition scheme, carbon atoms on the C-Mo_2C surface that are directly in contact with the adatom, are more negatively charged than in the pristine C-Mo_2C (-1.86 *e*), since they are able to acquire an additional charge from the adatom. The charge on molybdenum atoms that are the closest to the adatom remains almost unchanged, compared to the value in the unmodified surface ($Q_{Mo} = +1.57$ *e*), showing their little involvement into TM interaction with this surface.

However, in the case of Mo-Mo_2C systems, the relation between electronegativity and adatom's charge does not appear that straightforward. In these systems, the charge on molybdenum atoms in the topmost layer is noticeably affected by the presence of the adatom: according to Bader charges, a surface → TM charge transfer takes place through the surface atoms in direct contact with the adsorbate, since they become more positively charged than in pristine Mo-Mo_2C ($Q_{Mo} = +1.10$ *e*). Small change seen in the charge of carbon atoms in the sublayer, compared to the value of −2.52 *e* in the unmodified Mo-Mo_2C system, suggests that they are not involved into interaction with the adatoms.

The laterally averaged charge density difference (CDD) plots obtained from Eq. (7) are shown in Fig. 2. It illustrates that only upper layers of the support are affected by the presence of the adatom, regardless of the surface termination and nature of the adatom, while the charge distribution in the bottom layers remains almost unchanged, further evidencing the localized impact of the adatom on charge distribution in the system.

In the TM/C-Mo_2C system the majority of negative charge build-up takes place in the region close to the surface carbon atoms, and charge depletion is seen close to the location of the adatom. In contrast, negative charge accumulation is evident close to the adatom in the TM/Mo-Mo_2C system, while charge loss is observed for upper molybdenum atoms in the topmost layer of the support.

3.1.3. Changes in the work function.

Adsorption processes that involve the transfer of charge, have an impact on the system's work function, Φ, because electrons leaving the surface have to pass through the dipole layer of resulting interface. This change in the work function, in its turn, would affect the catalytic properties of the system, and particularly for hydrogen evolution reaction [4].

The change of the work function of a surface is affected by a layer of adsorbates, and, in general, the direction of the change can be predicted from the direction of the charge transfer between the adsorbate and the support. If the adsorbate is more electronegative than the substrate, it will gain charge (become more negative) and electrons will be transferred to the adsorbate layer, causing an excess of negative charge on the outside and an excess of positive charge on the inside of the surface. This would lead to a negative dipole, pointing toward the surface, and reinforcing the original surface dipole due to "spill out" of surface electrons, causing the work function to increase, *i.e.* $\Delta\Phi > 0$. If the substrate is more electronegative than the adsorbate, the adatoms would become positively charged upon the adsorption, so that the resulting negative dipole would be pointing toward the vacuum, and a decrease in work function would be expected, *i.e.* $\Delta\Phi < 0$.

Applied to the TM/Mo_2C systems, this formalism predicts a decrease of the work function in the TM/C-Mo_2C system upon adsorption of a single atom of Fe, Co, Ni or Cu, since they become positively charged (Table 1). Indeed, as it is seen in Fig. 3, adsorption of TM atoms has a significant effect on the values of Φ in the TM/C-Mo_2C systems, lowering them noticeably. On this termination the impact of the TM on the resulting work function is decreasing in the row: Fe > Ni > Co > Cu, in agreement with the trend seen from the Bader charge analysis for the decrease of adatom's charge (Table 1).

Conversely, in the TM/Mo-Mo_2C systems Bader charge analysis indicates that all adatoms are negatively charged (Table 1), and within the formalism described above, an increase in Φ would be expected. However, instead, a decrease in the work function is calculated, as seen in Fig. 3. The trend in ΔΦ for these systems evidences the biggest impact of the iron adatom on the work function, similarly to the case of TM/C-Mo_2C. Nevertheless, the effect of the other studied adatoms on the work function of Mo-terminated surface is different to the C-terminated surface and decreases in order: Fe > Co > Cu > Ni, not following the trend in negative charges calculated under the Bader scheme for the TM (Table 1). Also, the magnitude of the TM effect on the work function of Mo-terminated surface is reduced compared to that on the C-terminated $Mo_2C(0\,0\,1)$ plane.

This apparent anomalous decrease in the work function in presence of negatively charged adsorbates is not that uncommon in other

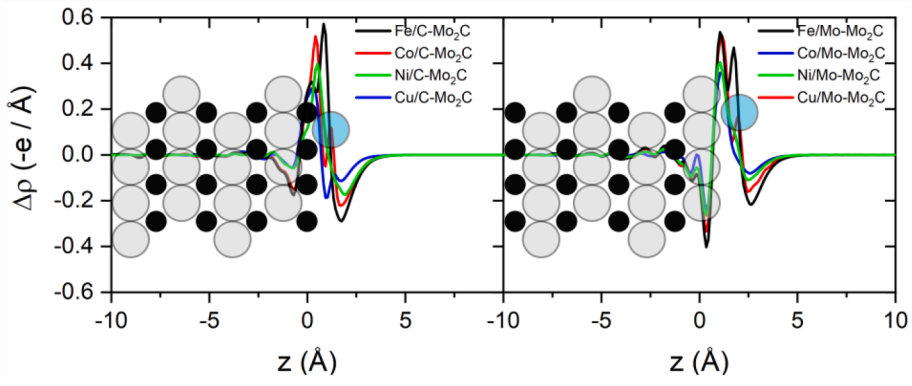

Fig. 2. Electron density profile, Δρ, for the adsorption of a single TM atom on model C-$Mo_2C(0\,0\,1)$ (left panel) and Mo-$Mo_2C(0\,0\,1)$ (right panel). Grey, black and blue spheres represent atoms of molybdenum, carbon and the TM, respectively. For each system vacuum region is cut at 10 Å to save space. Positive and negative values of Δρ correspond to charge build-up and depletion, respectively. (For interpretation of the references to colour in this figure legend, the reader is referred to the web version of this article.)

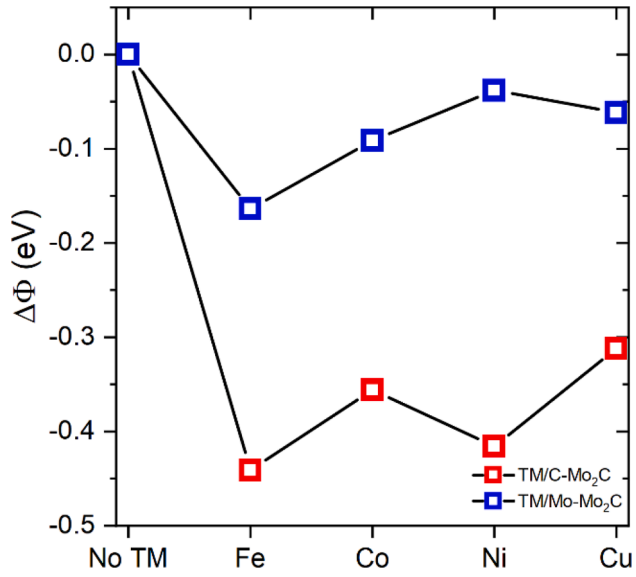

Fig. 3. Effect of TM adsorption on the work function of the C-Mo_2C and Mo-Mo_2C surfaces. **No TM** corresponds to the values for unmodified carbide (0 0 1) terminations.

adsorbate/substrate systems. A study of nitrogen adsorbed on tungsten (1 0 0) surface demonstrated that because nitrogen adatoms come very close to the surface, the adsorbate's electronic charge accumulation region is located beneath the spill out electron density of the surface, causing a small region of charge depletion outside the surface, and resulting in an overall reduced surface dipole, decreasing Φ [81]. Another study showed that in the I/Cu(1 1 1) system a weak dative covalent bond is formed by donation from I^- to Cu, causing a substantial shortening of the bond length [82]. Consequently, the dipole moment created by the negative charge and its positive charge inside the metal is significantly reduced as well, which was argued to be one of the factors behind the work function reduction in I/Cu(1 1 1) system, despite a charge transfer from the surface to the adatom.

Later works on adsorption of another halogens on Cu(1 1 1)[83] and Pt(1 1 1)[84] have also explained the "anomalous" decrease of the work function despite a negatively charged adatom, by a combination of charge transfer and polarization effects on the adsorbate layer. This approach is based on the decomposition of the total dipole change upon adsorption, $\Delta\mu_{BD}$, into two different contributions, a purely charge transfer-induced dipole moment from the adatom, $\Delta\mu_q$, and the polarization-induced dipole moment from the surface, $\Delta\mu_{pol}$, under a maximum charge transfer approximation [83,84]. This analysis, initially used in the works of Roman and Groß, and Gossenberger *et al.*, has been also applied to analyse an "anomalous" decrease of the work function of hafnium carbide covered with atomic oxygen [85].

In the present study, this method has been also applied,[83,84] and was used to analyse the anomalous change in the work function of Mo-Mo_2C surface seen in Fig. 3. Decomposition of $\Delta\mu_{BD}$ suggests that there is a similar contribution from the dipole moment induced purely by the charge transfer upon adatom adsorption on both terminations, indicating similar magnitude and same direction of the charge transfer. At the same time polarization-induced dipole moments on each surface differ. While in C-terminated $\Delta\mu_{pol}$ has the same sign as $\Delta\mu_q$, on Mo-terminated surfaces $\Delta\mu_{pol}$ and $\Delta\mu_q$ have different directions, as it can be seen in Figure S10. Therefore, under this approximation, the decrease in the work function upon adatom adsorption on Mo-terminated surfaces can be understood as a consequence of the different directions of the charge transfer-and polarization-induced dipole moments, counterbalancing each other, and giving rise to an overall small decrease in the work function of modified TM/Mo-Mo_2C systems. For the interested reader, details of this method can be found in the Section S2 of the Supplemental Information.

3.1.4. TM adatom-induced changes in electronic structure.

The analysis of the effect of the TM on the electronic structure of host systems was focused on the preferable sites for atomic hydrogen adsorption that are located in the contact region with the TM adatom, as indicated in Fig. S2 Specifically, an analysis has been performed of the normalized *s*- and *p*-Projected Density of States (PDOS) for C atoms in the topmost layer of the C-Mo_2C contacting the adsorbate, and the normalized *d*-PDOS for Mo atoms of the Mo-Mo_2C interacting with the adatom and the results are summarized in Fig. 4. Additionally, the electronic structure was also evaluated for the topmost-layer of carbon and molybdenum atoms not in contact with the TM on the TM/C-Mo_2C and TM/Mo-Mo_2C surfaces, respectively. In agreement with data on the charge redistribution and electron localization in these systems, the atoms not directly interacting with the TM do not undergo any significant change in their electronic structure.

Regardless of the nature of the adatom, the electronic structure of C atoms in its vicinity is affected by its presence, as it is shown in the left panel in Fig. 4. In this sense, the peak corresponding to *s*-band position of surface carbons in the unmodified C-Mo_2C located at −10.32 eV (Fig. S7), shifts further away from the Fermi lever: to −10.70 eV, −10.76 eV, −10.60 eV and −10.65 eV, for Fe/C-Mo_2C Co/C-Mo_2C, Ni/C-Mo_2C and Cu/C-Mo_2C, respectively. This shift is the result of the surface carbon simultaneous interaction with the TM adatom and molybdenum atom in the sublayer, as it is demonstrated for Co/C-Mo_2C system in the left panel in Fig. 4. Specifically, because of the separation between *d*-states of the subsurface molybdenum and the TM adatom interacting with the carbon, a split is seen for its *s*-states.

Another feature that is present in all systems is narrowing, and shifting to lower energies of carbon's *p*-states due to *pd*-interaction between C atom and the adatom and the appearance of a peak at ~ –3.8 eV in all TM/C-Mo_2C systems. This peak is present on the carbon *p*-states in unmodified C-Mo_2C but not as defined as upon TM adsorption (see Figs. S7 and 4) and it emerges regardless the nature of the TM adatom. Therefore, it can be treated as a characteristic feature of *p*-states of surface C atoms in the C-Mo_2C system, enhanced upon TM adatom presence. Importantly, the density of the carbon's *p*-states close to the Fermi level is not affected by the presence of the TM adatoms, which suggests that if presence of TM atoms on the surface has an impact on atomic H stability, the reasons behind it do not include adatom-induced variations in electronic structure of surface carbon atoms.

Right panel in Fig. 4 illustrates that the *d*-states of Mo atoms in contact with the TM on Mo-Mo_2C surface are affected by the adatoms. Similarly to carbon in the C-Mo_2C plane, an initial weakly defined peak at ~ –4.8 eV sharpens upon interaction with either Fe, Co, Ni or Cu. Importantly, for surface Mo atoms in contact with the TM, a shift of the *d*-band center further away from the Fermi level (downshift) is observed in respect to the value of −1.24 eV calculated for *d*-band center of Mo atoms in the topmost layer of the unmodified Mo-Mo_2C system. Depending on the nature of the adsorbate, the downshift in ε_d ranges from −0.05 eV for Cu/$MoMo_2C$ to −0.12 eV for Co/$MoMo_2C$.

The calculated downshift in the d-band center, $\Delta\varepsilon_d$, for TM/Mo-Mo_2C systems is in agreement with what would be expected from the *d*-band model, which predicts an upshift of the *d*-band center from a tensile strain and a downshift when a compressive strain is present [71,72,86]. According to this model, a shortened Mo–Mo bond would increase the overlap of atomic 4*d* orbitals, expanding and decreasing the population of the *d*-band, resulting in the *d*-band downshift to preserve the degree of *d*-band filling. Also, the small downshift agrees well with the fact that Mo atom is slightly more positively charged in the TM/Mo-Mo_2C systems, compared to the unmodified Mo-Mo_2C.

Interestingly, the Mo–Mo distances for Cu/Mo-Mo_2C and Ni/Mo-Mo_2C in the vicinity of the adatom are very close to the value of 3.18 Å in the unmodified Mo-Mo_2C, and, thus, practically no strain contributions to the changes in the ε_d position of molybdenum atoms in these systems

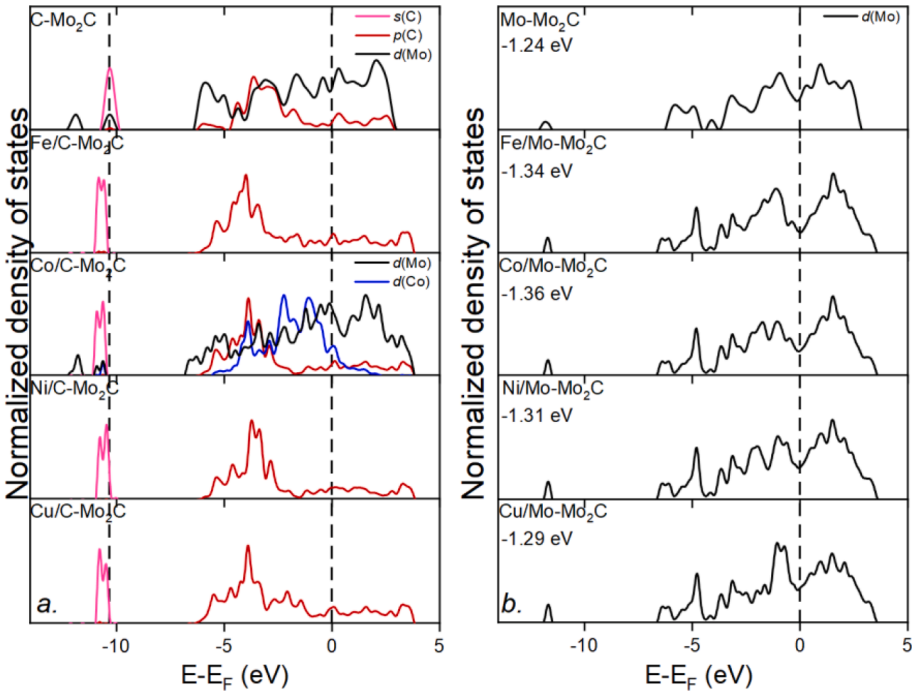

Fig. 4. Panel a: normalized *s*- and *p*-projected densities of states for C atom in the topmost layer in the vicinity of the TM adatom (as indicated in Fig. S2) of TM-decorated C-Mo_2C; for Co/C-Mo_2C system *d*-PDOS of molybdenum and cobalt, interacting with the C atom, are included as well as an example to demonstrate the impact of their *d* states on the splitting of carbon's *s*- state. Panel b: normalized *d*-projected densities of states for surface Mo atoms, affected by the TM adatom presence (as indicated in Fig. S2) of TM-decorated Mo-Mo_2C. *s*- and *p*-PDOS for surface C atoms of unmodified CMo_2C and *d*-PDOS–for surface Mo atoms of pristine Mo-Mo_2C are shown as well in the corresponding upper panels. For Mo-terminated surfaces the position of the *d*-band center is indicated.

are present. This and the fact that copper has the weakest impact on the Mo *d*-band center position, and Co has the strongest, indicate certain impact of the Mo → TM charge transfer on the position of the *d*-band for molybdenum. Thus, the observed $\Delta\varepsilon_d$ in the TM/Mo-Mo_2C systems are a combined result of the varying contributions from the compressive strain in Co and Fe, and ligand effect,[87] emerging from substrate–adatom interaction.

Overall, results clearly indicate that at the low coverages adsorbed Fe, Co, Ni and Cu atoms have a localized impact on the electronic properties of the atoms in each model surface, affecting only those of them that are adjacent to the adsorbate. Furthermore, the Φ lowering is seen in all systems, although of a different magnitude, depending on the surface termination and nature of the adsorbate. These changes open up a possibility to tune and optimize the reactivity of the complex TMC-based systems for target catalytic processes. Nonetheless, a reliable knowledge on how the TM adatoms affect HER activity of the Mo_2C support is still required in order to extract a conclusive picture. For this purpose, the impact of the TM-induced changes in the fundamental properties of the carbide polar terminations on H atom stability must be considered, and will be discussed in the next section.

3.2. Impact of TM adatoms on HER activity of $Mo_2C(001)$ surface polar terminations

TM-induced changes in fundamental properties of molybdenum carbide were further analysed in the context of their possible impact on the catalytic activity of the complex TM/Mo_2C systems toward hydrogen evolution reaction (HER). Experimentally, exchange current density, obtained from the Tafel approach from polarization curves,[4,5] or the magnitude of current density at a fixed overpotential can be used to numerically estimate HER catalytic activity of a given material. Based on these measurements a conclusion can be made on electrocatalytic activity of the materials of interest towards HER.

In acid media hydrogen evolution reaction starts with Volmer step, followed either by the Heyrovsky or Tafel steps:

$$H^+ + * + e^- \leftrightarrow H^*\text{(Volmer)}$$

$$H^* + H^+ + e^- \leftrightarrow * + H_2\text{(Heyrovsky)} \quad (9)$$

$$2H^* \leftrightarrow 2* + H_2\text{(Tafel)}$$

here * denotes the surface adsorption site. Thus, in course of HER, regardless of the steps it follows, the only expected reaction intermediate that directly interacts with the surface is atomic hydrogen. That is why its binding energy (HBE) on surface of a catalyst is one of the most commonly used descriptors of HER activity in acidic media for different materials, ranging from pure metals to complex composite systems [2,3,5,44].

In alkaline media, although water is the main reacting species, HBE can still be used as the descriptor for the catalytic activity toward HER [88,89]. This correlation can be understood by looking at the possible HER mechanism in the alkaline media, where it can either take the Volmer–Heyrovsky or Volmer–Tafel route:

$$H_2O + e^- + * \leftrightarrow H^* + OH^-\text{(Volmer)}$$

$$H^* + H_2O + e^- \leftrightarrow H_2 + OH^- + *\text{(Heyrovsky)} \quad (10)$$

$$2H^* \leftrightarrow 2* + H_2\text{(Tafel)}$$

Regardless of the mechanism, atomic hydrogen is still the only expected reaction intermediate, directly interacting with the surface of the catalyst, therefore, an optimal HBE is still an important factor, defining the balance between adsorption and desorption of the intermediate species in the alkaline media.

By plotting the exchange current density for a set of potential catalysts against a chosen descriptor of activity, a volcano-type curve is usually obtained. On it the optimal catalysts for HER is located in the proximity of an apex of the curve and characterized by a free energy for hydrogen adsorption approaching zero [5,90]. It must be noted here, that despite its apparent simplicity, the volcano curve method is sensitive to the calculation parameters, hydrogen coverages in the system and selected exchange correlation functional among others [12,44]. Additionally, this method of materials' screening tends to overlook certain intrinsic properties of the potential catalysts that can have an impact on their activity toward HER [91]. Nevertheless, despite its shortcomings, the volcano curve method is a valid tool for a preliminary HER activity assessment as evidenced by its successful application to estimate the

HER activity of a wide range of materials, from purely metallic systems [6] to more complex ones [3,41,92]. While not being able to predict accurately the values of exchange current density,[44] it, nevertheless, allows to establish activity trends and estimate changes in them caused by material modification.

Theoretical and experimental assessments of metal carbides' activity toward HER show an improvement, compared to their parent metals [3]. However, in general, HER activity of metal carbides is considered to be intermediate between the low activity exhibited by early transition metals and the highest activities inherent to Pt-group metals, because of strong atomic hydrogen interaction with the carbides' surfaces [2,38,62,93].

The HBE, in its turn, largely depends on the fundamental properties of the catalyst's surface, such as its work function and electronic structure [4,94]. It is, therefore, conceivable that the changes in fundamental properties of C- and Mo-Mo_2C systems, observed upon adsorption of Fe, Co, Ni and Cu atoms, will result in the departure of the HBE on these composite surfaces from the values on the unmodified surfaces. Consequently, this would lead to an HER activity of TM/Mo_2C different from that one of the unmodified molybdenum carbide.

Specifically, the tendency of TM adatoms to lower the work function would lead to a weaker hydrogen adsorption on both C- and Mo-Mo_2C surfaces. Additionally, changes in the *d*-band center position of molybdenum surface atoms Mo-Mo_2C, adjacent to the TM may destabilize H adsorption as well: *i.e.* the *d*-band center downshift, will cause a downward shift of antibonding states, formed upon coupling between the hydrogen *s*- and metal's *d*-states, leading to a weaker hydrogen–carbide bond. This in turn would predict a shift in the TM-modified carbide position on the volcano curve toward the weak adsorption shoulder, with respect to the initial position of Mo-terminated Mo_2C (001) surfaces, located in the left side of the volcano curve, the strong adsorbing side. Thus, the consequence of this shift will be an increase in theoretical exchange current density and an improvement of HER activity on TM-modified carbide surfaces compared to that of the pristine parent systems.

To verify this hypothesis, adsorption of a single H atom was also studied on the TM-modified polar terminations of Mo_2C(001) surface. As it was stated above, on C-Mo_2C hydrogen preferably occupies Top-C site with HBE −0.87 eV and on Mo-Mo_2C it sits on Ehcp-1 site (Fig. 1) with $E_{ads,H} = -1.15$ eV. H adsorption on the same sites was analysed on the TM-modified surfaces, and two modes were considered: adsorption on the most stable site in the proximity of TM adatom, and adsorption on the most stable site of the surface, located at a large distance (at least 4.5 Å) from the adatom, as it is shown in Fig. 5.

Fig. 5 demonstrates that H atom adsorbed in the proximity of the TM adatom, depending on the surface termination, is able to interact with the C and Mo atoms in direct contact with the TM adatom. Adsorption characteristics for atomic H are summarized in Table 2, and suggest that as the result of its interaction with these surface atoms, a destabilization of H adsorption is seen, as HBE becomes more positive, as expected from tendencies discussed above. In all cases changes in atomic hydrogen adsorption depend more on the nature of the TM adatom than on the termination of the carbide surface. Indeed, in systems where Co or Fe atom is present the weakening of H–carbide bond is ~ 0.3 eV, regardless of the termination, while the H–carbide interaction is less affected by Cu or Ni atom presence. The observed changes in the HBE on Fe/Mo_2C agree well with work function lowering seen in Fig. 3, where the biggest effect on the work function of both terminations was seen upon Fe adsorption.

In all TM/Mo_2C systems, the surface–hydrogen distances remain virtually the same and are close to those seen on C- and Mo-Mo_2C surfaces. The biggest change seen for H atom in the vicinity of a TM adatom is its total net charge, Q_H, that compared to its charge on the unmodified terminations, becomes slightly less positive on TM/C-Mo_2C and more positive – on TM/Mo-Mo_2C (Table 2). On C-Mo_2C it might be the consequence of surface carbon atoms already acquiring charge from the

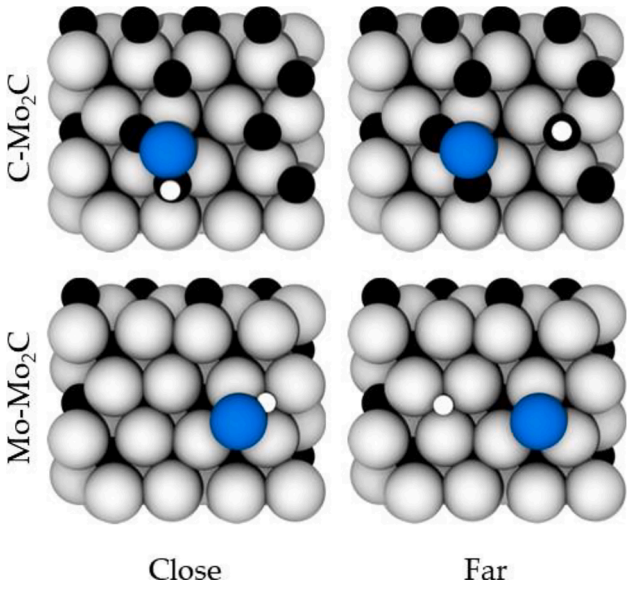

Fig. 5. Top view on TM/C-Mo_2C(001) and TM/Mo-Mo_2C(001) with single H atom adsorbed close to the TM adatom at a distance. Molybdenum, carbon, TM and H atoms are represented by silver, black, blue and white spheres, respectively. (For interpretation of the references to colour in this figure legend, the reader is referred to the web version of this article.)

TM (see Table 1) and thus, reducing H → C charge transfer, compared to that in the unmodified system. On the Mo-Mo_2C, atomic hydrogen interacts with three surface molybdenum atoms, two of which are participating in the Mo → TM charge transfer, becoming slightly more positive than corresponding Mo atoms in the pristine Mo-terminated (001) surface. Thus, in this case hydrogen is not able to acquire the total charge it has upon adsorption on pristine Mo-Mo_2C surface. Importantly, no charge transfer takes place between the TM and hydrogen (Fig. S3), pointing to no direct interaction between the adatom and hydrogen.

Additionally, on the C-Mo_2C surface both hydrogen atom and TM adatom are charged positively on this termination, which could lead to repulsive interactions, weakening hydrogen adsorption. In support of this hypothesis, a noticeable displacement of hydrogen away from the TM adatom is seen in all TM/C-Mo_2C systems, not present on the TM/Mo-Mo_2C surfaces (Fig. S4).

Nevertheless, regardless of the charge on the metal adatoms, the downshift of *d*-states of surface molybdenum atoms caused by the TM species is expected to weaken the H–surface interaction on the TM/Mo-Mo_2C surfaces. Finally, decrease of the work function of C- and Mo-Mo_2C upon TM atom adsorption is another important factor that has a destabilizing effect on the H–surface interaction as well, regardless of the termination of the carbide.

Since the effect of a single TM adatom presence on fundamental properties of the Mo_2C terminations is very localized, it can be assumed that hydrogen adsorption on surface sites, located far from the modification site would remain almost unaffected. Indeed, as the data in Table 2 indicates, HBE values for H atom, adsorbed at a larger distance from the adatom are very close to those on the corresponding unmodified Mo_2C(001) polar terminations.

Additionally, H atom was placed on top of the TM adatom in each studied system, to estimate its stability on this unique side. In all cases H adsorption on the carbide's surface is more stable, than on the adatoms themselves, regardless of the TM adatom and surface termination. Therefore, at 1/16 ML surface coverage HER activities of the TM/Mo_2C surfaces are defined by interaction of atomic hydrogen with the carbide.

To better understand the impact of the observed TM-induced HBE weakening on the HER activity of the resulting TM/Mo_2C materials, free

energies for hydrogen adsorption, ΔG_{H^*}, were calculated for all considered systems as proposed by Nørskov *et al.* [5] and are summarized in Fig. 6. In the same figure ΔG_{H^*} value for Pt(1 1 1), calculated using the same model setup as described in Section 2, is included for the reference. It can be seen that on both terminations the presence of Fe and Co leads to the biggest shift in ΔG_{H^*} toward zero. In case of C-terminated surface the resulting free energies in Fe/C-Mo_2C and Co/ C-Mo_2C systems are slightly more positive than that of Pt(1 1 1), the best known single metal catalyst for HER. Bearing in mind that on the volcano curve Pt is located on its strong-binding side, H adsorption on Fe/C-Mo_2C and Co/C-Mo_2C weaker than on Pt(1 1 1) suggests that these systems would demonstrate good catalytic activity toward HER, outperforming the rest of the studied systems.

In the realistic system, however, it is difficult, if not impossible, to isolate a specific termination of the carbide. Therefore, HER activity of Mo_2C modified with either of the TMs would be a function of statistical distribution of C- and Mo-active sites on the surface. Thus, HER activity of either Fe- or Co-modified Mo_2C would be higher than that of unmodified phase, but lower than the activity of platinum. Compared to these two modifying metals, the effect of either Ni or Cu on catalytic properties of the carbide toward hydrogen evolution would be even smaller, however, still resulting in the better activity than of the unmodified carbide.

Indeed, in the context of experimentally studied systems, comparison of the changes in $E_{ads,H}$ to the trend of activities seen for TM-modified Mo_2C in alkaline media, Co-Mo_2C > Ni-Mo_2C > Fe-Mo_2C > Cu-Mo_2C > Mo_2C,[30] reveals certain similarities. Specifically, Co has the biggest theoretically estimated impact on the HBE, and experimentally evaluated activity of the Co-modified Mo_2C is the highest, compared to the rest of the systems. Also, copper has the smallest effect on the HBE on the TM-modified Mo-Mo_2C and its impact on HBE on the TM/C-Mo_2C is smaller than that of Co and Fe, but only slightly higher than Ni. However, judging exclusively from the HBE weakening, Fe-modified Mo_2C should be more active than Ni-Mo_2C, while experimental results evidence the contrary. Clearly, other factors besides the ones discussed here affect the overall HER activity of TM-modified Mo_2C materials. Therefore, while TM-induced changes in the HBE definitely have an impact on HER activity of the resulting composite materials, TM presence in the system may have other effects on the activity of the TM/Mo_2C materials that are overlooked by the theoretical model.

A possible reason can be that in this study decoration by a single TM atom has been considered of the well-defined polar terminations of the carbide, for which no reliable synthesis protocols exist yet. In the real systems the coverage of the TM adatoms can be much higher and will play an important role. Specifically, at higher TM coverages more surface atoms of the carbide will be affected by the presence of the TM species, affecting the average HBE on these surfaces. Furthermore, at high TM coverages some, if not most of the carbide sites will become unavailable, and hydrogen adsorption will take place mostly on alternative sites formed by the adatoms and their electronic structure would play an increasingly important role.

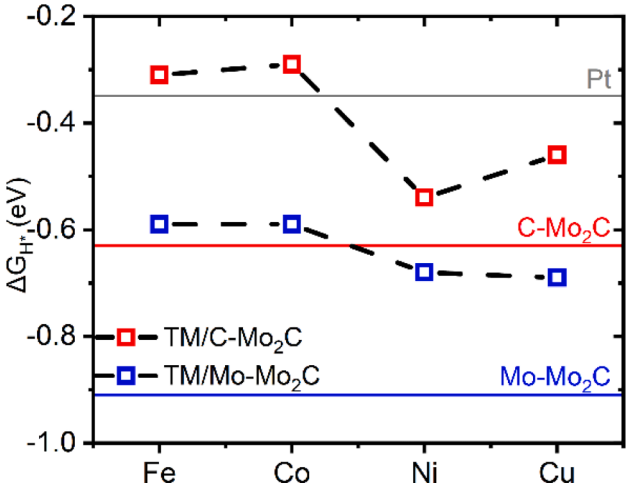

Fig. 6. ΔG_{H^*} values on TM/Mo_2C, calculated as in ref. [5]. Grey, red and blue horizontal lines indicate ΔG_{H^*} on Pt(1 1 1), C-Mo_2C and Mo-Mo_2C, respectively. (For interpretation of the references to colour in this figure legend, the reader is referred to the web version of this article.)

Also, the present study has not considered the effect of insertion of a molybdenum atom into crystalline lattice of the carbide that also may affect atomic H stability on the modified Mo_2C(0 0 1) terminations, contributing to the changes in their HER activity. Finally, the presence of electrolyte in the system was not taken into account, however, it may have an additional impact on fundamental properties of the TM/Mo_2C systems, affecting their HER activity.

3.3. Stability of adatoms on polar terminations of Mo_2C(0 0 1) surface

An important characteristic of a catalyst is its stability under the working conditions. Here the stability of the TM/Mo_2C materials in was estimated using the method proposed by Anićijević et al. [95] It is based on a galvanic cell using electrolyte containing TM^{z+} ions with a unit activity, the TM/Mo_2C material employed as an anode and the corresponding TM metal – as a cathode. Electron transfer process from the anode to the cathode can be seen as a subtraction of *z* electrons from the TM adatom with consecutive desorption of the adatom from the Mo_2C surface. This desorption can be achieved when an energy equal by value but contrary by sign to TM adatom adsorption energy is applied.

The following process, when formed TM^{z+} ion is transferred to the electrolyte, is associated with the enthalpy of solvation. After that a TM^{z+} ion leaves the solvation shell in the proximity of TM cathode, reduces to neutral TM atom and gets incorporated into the cathode, releasing the energy equal to bulk cohesion energy of TM.

Thus, the total work required for the described electrochemical process to take place is a difference between the adsorption energy of the TM atom on a given termination of the Mo_2C(0 0 1) surface and bulk cohesion energy for the corresponding TM (see Table 1).

The electromotive force, EMF, of the cell described here can be obtained as follows:

$$EMF = \frac{E_{Ads,TM} - E_c}{zF} \quad (12)$$

where F is Faraday constant and z – number of transferred electrons, which for all transition metals considered in this work was equal 2.

Replacing TM electrode with Standard Hydrogen Electrode would result in the EMF of this cell being equal to the standard redox potential of the TM ($E^o_{TM^{z+}/TM}$) also listed in Table 1. A potential at which a given TM adatom will be removed from the surface (E_{des}) can be obtained by combining EMFs of these two cells:

$$E_{des} = E^o_{TM^{z+}/TM} - \frac{E_{Ads,TM} - E_c}{zF} \quad (13)$$

In all cases, regardless of the TM adatom nature or the support's termination, calculated adsorption energies for TMs were more negative than the corresponding cohesion energies. Thus, the $E_{Ads,TM} - E_c$ term in eq. (13) remains negative for all TM/Mo_2C systems. This leads to E_{des} being more positive than $E^o_{TM^{z+}/TM}$ term and indicates a good stability of the considered TM/Mo_2C systems in the potential window of HER.

4. Conclusions

A theoretical study has been conducted on single atom adsorption of Fe, Co, Ni and Cu on polar terminations of β-Mo_2C(0 0 1) surface. A detailed analysis of adsorption characteristics, including energies and geometries of TM/Mo_2C systems has been performed. An in-depth study

of adatom-induced variations in electronic properties of molybdenum carbide (001) surface provides molecular-level insights into termination-specific interactions of the TM with β-Mo_2C.

At the low coverage of 1/16 ML considered here, the adsorption of a single atom of either of the TMs leads to a noticeable shift in the properties of model carbide surface terminations. Specifically, on Mo-terminated surface the shift of the *d*-band center position further away from the Fermi level is seen for molybdenum atoms in the topmost layer, that are directly in contact with the adatom, and on both terminations the charge redistribution in the contact region takes place, causing lowering in their Φ. This decrease in the work function is the result of the termination-dependent contributions of charge transfer-and polarization-induced dipole moments to the total dipole change upon adatom adsorption.

In the context of HER activity of TM/Mo_2C compared to that of the unmodified Mo_2C, TM adatoms play a many-fold role. On both terminations, they induce a work function lowering, and affect charge transfer between the carbide's surface atoms and hydrogen, reducing HBE. On Mo-Mo_2C, additionally to these effects, the TM-induced ε_d downshift further contributes to atomic H adsorption destabilization. Obtained data suggest that Co– and Fe-modified carbide would exhibit better catalytic properties toward HER compared to Ni- and Cu-modified Mo_2C as well as to the bare (pure) carbide, in a partial agreement with experimentally observed trends of activity.

Thus, the obtained results pave the path toward better understanding of complex TM/TMC systems as alternative to platinum-based catalysts for processes meaningful to the field of sustainable energy conversion and storage.

CRediT authorship contribution statement

Andrey A. Koverga: Conceptualization, Methodology, Investigation, Writing – original draft. **Ana M. Gómez-Marín:** Conceptualization, Validation, Methodology, Investigation, Writing – review & editing. **Elizabeth Flórez:** Methodology, Validation, Writing – review & editing. **Edson A. Ticianelli:** Project administration, Methodology, Validation, Supervision, Writing – review & editing.

Declaration of Competing Interest

The authors declare the following financial interests/personal relationships which may be considered as potential competing interests: Andrey Koverga reports financial support was provided by State of Sao Paulo Research Foundation.

Data availability

Data will be made available on request.

Acknowledgments

The authors would like to thank Fundação de Amparo a Pesquisa do Estado de São Paulo (FAPESP – Procs. 2020/11947-2 and 2019/22183-6), Brazil, for financial support and the Center for Mathematical Sciences Applied to Industrial (CeMEAI) for providing the computational resources for the research. Authors also express their gratitude to Universidad de Medellin.

Appendix A. Supplementary material

Supplementary data to this article can be found online at https://doi.org/10.1016/j.apsusc.2023.157498.

References

[1] B. Wolter, M.G. Pullen, M. Baudisch, M. Sclafani, M. Hemmer, et al., Phys. Rev. X 5 (2) (2015), 021034.
[2] D.V. Esposito, S.T. Hunt, Y.C. Kimmel, J.G. Chen, J. Am. Chem. Soc. 134 (6) (2012) 3025–3033.
[3] R. Michalsky, Y.-J. Zhang, A.A. Peterson, ACS Catal. 4 (5) (2014) 1274–1278.
[4] S. Trasatti, J. Electroanal. Chem. Interfacial Electrochem. 39 (1) (1972) 163–184.
[5] J.K. Nørskov, T. Bligaard, A. Logadottir, J.R. Kitchin, J.G. Chen, S. Pandelov, U. Stimming, J. Electrochem. Soc. 152 (3) (2005) J23–J26.
[6] J. Greeley, T.F. Jaramillo, J. Bonde, I. Chorkendorff, J.K. Nørskov, Nat. Mater. 5 (11) (2006) 909–913.
[7] W. Sheng, M. Myint, J.G. Chen, Y. Yan, Energ. Environ. Sci. 6 (5) (2013) 1509–1512.
[8] R.B. Levy, M. Boudart, Science 181 (4099) (1973) 547–549.
[9] S. Wirth, F. Harnisch, M. Weinmann, U. Schröder, Appl Catal B 126 (25) (2012) 225–230.
[10] H. Vrubel, X. Hu, *Angewandte Chemie Int. Ed.* **2012,** *51* (51), 12703-12706.
[11] H. Prats, J.J. Piñero, F. Viñes, S.T. Bromley, R. Sayós, F. Illas, Chem. Commun. 55 (85) (2019) 12797–12800.
[12] A.A. Koverga, E. Florez, L. Dorkis, J.A. Rodriguez, J. Phys. Chem. C 123 (14) (2019) 8871–8883.
[13] J. Gan, F. Li, Y. Tang, Q. Tang, ChemSusChem 13 (22) (2020) 6005–6015.
[14] J.R. Morse, M. Juneau, J.W. Baldwin, M.D. Porosoff, H.D. Willauer, J. CO_2 Util. 35 (2020) 38–46.
[15] T. Gu, R. Sa, L. Zhang, D.-S. Li, R. Wang, Appl. Catal. B 296 (5) (2021), 120360.
[16] Z. Nie, Z. Tang, D. Jiao, M. Yuan, J. Zhao, Q. Lai, Y. Liang, ChemCatChem 2022 (1885) e20210.
[17] W. Zhao, Z. Guan, D. Li, B. Wang, M. Fan, R. Zhang, ACS Appl. Mater. Interfaces 14 (17) (2022) 19491–19504.
[18] D. Merki, X. Hu, Energ. Environ. Sci. 4 (10) (2011) 3878–3888.
[19] D. Merki, H. Vrubel, L. Rovelli, S. Fierro, X. Hu, Chem. Sci. 3 (8) (2012) 2515–2525.
[20] W.F. Chen, J.T. Muckerman, E. Fujita, Chem. Commun. 49 (79) (2013) 8896–8909.
[21] W.F. Chen, C.H. Wang, K. Sasaki, N. Marinkovic, W. Xu, J.T. Muckerman, Y. Zhu, R.R. Adzic, Energy Environ. Sci. 6 (2013) 943–951.
[22] H. Vrubel, T. Moehl, M. Grätzel, X. Hu, Chem. Commun. 49 (79) (2013) 8985–8987.
[23] D.H. Youn, S. Han, J.Y. Kim, J.Y. Kim, H. Park, S.H. Choi, J.S. Lee, ACS Nano 8 (5) (2014) 5164–5173.
[24] Y.N. Regmi, G.R. Waetzig, K.D. Duffee, S.M. Schmuecker, J.M. Thode, B. M. Leonard, J. Mater. Chem. A 3 (18) (2015) 10085–10091.
[25] A.M. Gómez-Marín, E.A. Ticianelli, Electrochim. Acta 220 (2016) 363–372.
[26] S. Wu, M. Chen, W. Wang, J. Zhou, X. Tang, D. Zhou, C. Liu, Carbon 171 (2021) 385–394.
[27] C. Wan, B.M. Leonard, Chem. Mater. 27 (12) (2015) 4281–4288.
[28] K. Xiong, L. Li, L. Zhang, W. Ding, L. Peng, Y. Wang, Z. Wei, J. Mater. Chem. A 3 (5) (2015) 1863–1867.
[29] A.M. Gómez–Marín, E.A. Ticianelli, Appl. Catal. B 209 (2017) 600–610.
[30] A.A. Koverga, A.M. Gómez-Marín, L. Dorkis, E. Flórez, E.A. Ticianelli, ACS Appl. Mater. Interfaces 12 (24) (2020) 27150–27156.
[31] M. Watanabe, M. Horiuchi, S. Motoo, J. Electroanal. Chem. Interfacial Electrochem. 250 (1) (1988) 117–125.
[32] D. Mey, S. Brunet, C. Canaff, F. Maugé, C. Bouchy, F. Diehl, J. Catal. 227 (2) (2004) 436–447.
[33] Y. Kwon, T.J. Hersbach, M. Koper, Top. Catal. 57 (14) (2014) 1272–1276.
[34] C. Tsai, K. Chan, J.K. Nørskov, F. Abild-Pedersen, Cat. Sci. Technol. 5 (1) (2015) 246–253.
[35] X. Song, M. Dong, Y. Li, Y. Wu, Y. Sun, G. Yuan, Y. Li, Chem. Phys. Lett. 761 (2020), 138085.
[36] A.A. Koverga, A.M. Gomez-Marin, E. Flórez, J. Phys. Chem. C 126 (24) (2022) 10167–10180.
[37] A.A. Koverga, E. Florez, A.M. Gomez-Marin, Appl. Surf. Sci. 608 (2023), 155137.
[38] D.V. Esposito, J.G. Chen, Energ. Environ. Sci. 4 (10) (2011) 3900.
[39] T.G. Kelly, S.T. Hunt, D.V. Esposito, J.G. Chen, Int. J. Hydrogen Energy 38 (14) (2013) 5638–5644.
[40] D.D. Vasic Anicijevic, V.M. Nikolic, M.P. Marceta-Kaninski, I.A. Pašti, Int. J. Hydrogen Energy 38 (2013) 1607.
[41] D.D. Vasić, I.A. Pašti, S.V. Mentus, Int. J. Hydrogen Energy 38 (12) (2013) 5009–5018.
[42] S. Posada-Perez, F. Viñes, J.A. Rodriguez, F. Illas, J. Chem. Phys. 143 (11) (2015), 114704.
[43] A.A. Koverga, E. Florez, L. Dorkis, J.A. Rodriguez, PCCP 22 (24) (2020) 13666–13679.
[44] A.A. Koverga, E. Florez, C. Jimenez-Orozco, J.A. Rodriguez, Electrochim. Acta 368 (2021), 137598.
[45] A.A. Koverga, E. Florez, C. Jimenez-Orozco, J.A. Rodriguez, PCCP 23 (36) (2021) 20255–20267.
[46] J.R. dos Santos Politi, F. Viñes, J.A. Rodriguez, F. Illas, PCCP 15 (30) (2013) 12617.
[47] K. Page, J. Li, R. Savinelli, H.N. Szumila, J. Zhang, J.K. Stalick, R. Seshadri, Solid State Sci. 10 (11) (2008) 1499–1510.
[48] H.W. Hugosson, U. Jansson, B. Johansson, O. Eriksson, Chem. Phys. Lett. 333 (6) (2001) 444–450.
[49] G. Kresse, J. Hafner, Phys. Rev. B 47 (1) (1993) 558–561.
[50] G. Kresse, J. Hafner, Phys. Rev. B 49 (20) (1994) 14251–14269.
[51] G. Kresse, J. Furthmuller, Phys. Rev. B 54 (16) (1996) 11169–11186.

[52] G. Kresse, J. Furthmuller, Comput. Mater. Sci. 6 (1996) 15–50.
[53] J.P. Perdew, K. Burke, M. Ernzerhof, Phys. Rev. Lett. 77 (18) (1996) 3865–3868.
[54] P.E. Blöchl, Phys. Rev. B 50 (24) (1994) 17953–17979.
[55] G. Kresse, D. Joubert, Phys. Rev. B 59 (3) (1999) 1758–1775.
[56] S. Grimme, J. Comput. Chem. 25 (12) (2004) 1463–1473.
[57] S. Grimme, J. Antony, S. Ehrlich, H. Krieg, J. Chem. Phys. 132 (15) (2010), 154104.
[58] H.J. Monkhorst, J.D. Pack, Phys. Rev. B 13 (12) (1976) 5188–5192.
[59] M. Methfessel, A.T. Paxton, Phys. Rev. B 40 (6) (1989) 3616–3621.
[60] J.R. Kitchin, J.K. Nørskov, M.A. Barteau, J.G. Chen, Catal. Today 105 (1) (2005) 66–73.
[61] S. Posada-Perez, F. Viñes, P.J. Ramirez, A.B. Vidal, J.A. Rodriguez, F. Illas, PCCP 16 (28) (2014) 14912–14921.
[62] S. Posada-Perez, F. Viñes, R. Valero, J.A. Rodriguez, F. Illas, Surf. Sci. 656 (2017) 24–32.
[63] R.F.W. Bader, Atoms in Molecules: A Quantum theory, Oxford University Press, Oxford, U.K., 1990.
[64] G. Henkelman, A. Arnaldsson, H. Jónsson, Comput. Mater. Sci 36 (3) (2006) 354–360.
[65] S. Otani, Y. Ishizawa, J. Cryst. Growth 154 (1–2) (1995) 202–204.
[66] A. Vojvodic, Catal. Lett. 142 (6) (2012) 728–735.
[67] G.-Q. Yu, B.-Y. Huang, X. Chen, D. Wang, F. Zheng, X.-B. Li, J. Phys. Chem. C 123 (36) (2019) 21878–21887.
[68] J. Wan, Q. Liu, T. Wang, H. Yuan, P. Zhang, X. Gu, Solid State Commun. 284–286 (2018) 25–30.
[69] A.F. Guillermet, J. Häglund, G. Grimvall, Phys. Rev. B 45 (20) (1992) 11557–11567.
[70] F. Viñes, C. Sousa, P. Liu, J.A. Rodriguez, F. Illas, J. Chem. Phys. 122 (17) (2005), 174709.
[71] X. Zheng, L. Li, J. Li, Z. Wei, PCCP 21 (6) (2019) 3242–3249.
[72] E.M. Dietze, H. Grönbeck, ChemPhysChem 21 (21) (2020) 2407–2410.
[73] K. Yan, T.A. Maark, A. Khorshidi, V.A. Sethuraman, A.A. Peterson, P.R. Guduru, Angew. Chem. 128 (21) (2016) 6283–6289.
[74] K. Yan, S. K.; Kim, A. Khorshidi, P. R. Guduru, A. A. Peterson, *J. Phys. Chem. C* **2017,** *121* (11), 6177-6183.
[75] R. A. Campbell, J. A.; Rodriguez, D. W. Goodman, *Physical Review B* **1992,** *46* (11), 7077-7087.
[76] I.A. Pašti, S.V. Mentus, Russ. J. Phys. Chem. A 83 (9) (2009) 1531–1536.
[77] I.A. Pašti, S.V. Mentus, J. Alloy. Compd. 497 (1–2) (2010) 38–45.
[78] D.D.V. Aničijević, V.M. Nikolić, M.P.M. Kaninski, I.A. Pašti, Int. J. Hydrogen Energy 40 (18) (2015) 6085–6096.
[79] IUPAC Gold Book. http://goldbook.iupac.org/I03046.html (accessed Apr. 2023).
[80] A.L. Allred, J. Inorg. Nucl. Chem. 17 (3–4) (1961) 215–221.
[81] A. Michaelides, P. Hu, M.-H. Lee, A. Alavi, D.A. King, Phys. Rev. Lett. 90 (24) (2003), 246103.
[82] P.S. Bagus, D. Kafer, G. Witte, C. Woll, Phys. Rev. Lett. 100 (2008), 126101.
[83] T. Roman, A. Groß, Phys. Rev. Lett. 110 (15) (2013), 156804.
[84] F. Gossenberger, T. Roman, K. Forster-Tonigold, A. Groß, Beilstein J. Nanotechnol. 5 (2014) 152–161.
[85] J. Wang, S.-Q. Wang, Appl. Surf. Sci. 357 (2015) 1046–1052.
[86] T.A. Maark, A.A. Peterson, J. Phys. Chem. C 118 (8) (2014) 4275–4281.
[87] J.R. Kitchin, J.K. Nørskov, M.A. Barteau, J.G. Chen, Phys. Rev. Lett. 93 (15) (2004), 156801.
[88] W. Sheng, Z. Zhuang, M. Gao, J. Zheng, J.G. Chen, Y. Yan, Nat. Commun. 6 (1) (2015) 1–6.
[89] J. Zheng, W. Sheng, Z. Zhuang, B. Xu, Y. Yan, Sci. Adv. 2 (3) (2016) e1501602.
[90] T. Bligaard, J.K. Nørskov, S. Dahl, J. Matthiesen, C.H. Christensen, J. Sehested, J. Catal. 224 (1) (2004) 206–217.
[91] P. Quaino, F. Juarez, E. Santos, W. Schmickler, Beilstein J. Nanotechnol. 5 (2014) 846–854.
[92] M.E. Björketun, A.S. Bondarenko, B.L. Abrams, I. Chorkendorff, J. Rossmeisl, PCCP 12 (35) (2010) 10536–10541.
[93] R. Michalsky, Y.-J. Zhang, A.J. Medford, A.A. Peterson, J. Phys. Chem. C 118 (24) (2014) 13026–13034.
[94] B. Hammer, J.K. Nørskov, Surf. Sci. 343 (3) (1995) 211–220.
[95] D.D.V. Aničijević, V.M. Nikolić, M.P.M. Kaninski, I.A. Pašti, Int. J. Hydrogen Energy 38 (36) (2013) 16071–16079.